

Measurement of the $e^+e^- \rightarrow \pi^+\pi^-$ cross section with the CMD-2 detector in the 370-520 MeV c.m. energy range

R. R. Akhmetshin^a, V. M. Aulchenko^{a,b}, V. Sh. Banzarov^a, L. M. Barkov^{a,b},
 N. S. Bashtovoy^a, A. E. Bondar^{a,b}, D. V. Bondarev^{a,b}, A. V. Bragin^a,
 S. K. Dhawan^d, S. I. Eidelman^{a,b}, D. A. Epifanov^a, G. V. Fedotov^{a,b},
 N. I. Gabyshev^a, D. A. Gorbachev^a, A. A. Grebenuk^a, D. N. Grigoriev^{a,b},
V. W. Hughes^d, F. V. Ignatov^a, S. V. Karpov^a, V. F. Kazanin^{a,b},
 B. I. Khazin^{a,b}, I. A. Koop^{a,b}, P. P. Krokovny^{a,b}, A. S. Kuzmin^{a,b},
 I. B. Logashenko^{a,c}, P. A. Lukin^{a,b}, A. P. Lysenko^a, K. Yu. Mikhailov^a,
 A. I. Milshtein^{a,b}, I. N. Nesterenko^{a,b}, M. A. Nikulin^a, V. S. Okhapkin^a,
 A. V. Otboev^a, E. A. Perevedentsev^{a,b}, A. S. Popov^a, S. I. Redin^a,
 B. L. Roberts^c, N. I. Root^a, A. A. Ruban^a, N. M. Ryskulov^a, A. G. Shamov^a,
 Yu. M. Shatunov^a, B. A. Schwartz^{a,b}, A. L. Sibidanov^{a*}, V. A. Sidorov^a,
 A. N. Skrinsky^a, V. P. Smakhtin^f, I. G. Snopkov^a, E. P. Solodov^{a,b},
J. A. Thompson^e, Yu. V. Yudin^a, A. S. Zaitsev^{a,b}, S. G. Zverev^a

^a*Budker Institute of Nuclear Physics, 630090, Novosibirsk, Russia*

^b*Novosibirsk State University, 630090, Novosibirsk, Russia*

^c*Boston University, Boston, MA 02215, USA*

^d*Yale University, New Haven, CT 06511, USA*

^e*University of Pittsburgh, Pittsburgh, PA 15260, USA*

^f*Weizmann Institute of Science, 76100, Rehovot, Israel*

Abstract

The cross section of the process $e^+e^- \rightarrow \pi^+\pi^-$ has been measured at the CMD-2 detector in the 370-520 MeV center-of-mass (c.m.) energy range. A systematic uncertainty of the measurement is 0.7%. Using all CMD-2 data on the pion form factor, the pion electromagnetic radius was calculated. The cross section of muon pair production was also determined.

*e-mail: A.L.Sibidanov@inp.nsk.su

1 Introduction

Study of the process $e^+e^- \rightarrow \pi^+\pi^-$ provides important information about the pion electromagnetic form factor, which describes its internal structure and is predicted by various theoretical models. Accurate cross section measurement is necessary for a more precise determination of the hadronic contribution to the muon anomalous magnetic moment, which is given in perturbation theory by the dispersion integral [1]:

$$a_\mu^{\text{had,LO}} = \frac{m_\mu^2}{12\pi^3} \int_{4m_\pi^2}^{\infty} ds \frac{\sigma^{(0)}(e^+e^- \rightarrow \text{hadrons}) \hat{K}(s)}{s}, \quad (1)$$

where $\hat{K}(s)$ is a function monotonously rising from 0.63 at the threshold of pion pair production $s = 4m_\pi^2$ up to 1 at $s \rightarrow \infty$, where s is the total c.m. energy squared. Since the kernel $\hat{K}(s)/s$ in the integral enhances a contribution from the low energy region, particularly important is precise knowledge of the cross section of the process $e^+e^- \rightarrow \pi^+\pi^-$, which is dominating below 1 GeV. Furthermore, this cross section is needed to test the relation between the two-pion spectral function in e^+e^- annihilation and τ decays, based on conserved vector current and SU(2) symmetry [2].

For analysis we use a data sample of 56 nb^{-1} collected with the CMD-2 detector at the electron-positron collider VEPP-2M [3] at 10 c.m. energy points from 370 MeV to 520 MeV. During the experiment about one million events were recorded.

A general-purpose cryogenic magnetic detector (CMD-2) [4] consists of a tracking system, barrel and endcap electromagnetic calorimeters based on CsI and BGO crystals, respectively, and a muon-range system. The tracking system consists of a drift chamber with jet-like cells and two layers of a proportional Z-chamber inside a thin superconductive solenoid with 1 T magnetic field.

During data taking two independent triggers were used: “charged” and “neutral”. The “charged” trigger required at least one track in the drift chamber while the “neutral” one used information about energies and positions of clusters in the CsI calorimeter.

2 Event selection

About 1.1×10^5 collinear events were selected from raw data by applying the following selection criteria:

- There is a “charged” trigger in event.
- Two particles with opposite charges were found in the drift chamber.
- $\rho_{1,2} < 0.3 \text{ cm}$, where ρ is a particle impact parameter relative to the beam axis.
- $|Z_{1,2}| < 7 \text{ cm}$, where Z is a coordinate at the point of the closest approach to the beam line.

- $|\Delta\phi| = |\pi - |\phi_1 - \phi_2|| < 0.15$, where ϕ is an azimuthal track angle.
- $|\Delta\theta| = |\pi - (\theta_1 + \theta_2)| < 0.25$, where θ is a polar track angle.
- Momentum of a final particle, P , should be smaller than 350 MeV/ c , and the transverse momentum $P \times \sin\theta$ should be larger than 90 MeV/ c . The last condition ensures a constant “charged” trigger efficiency. At lower momentum the efficiency starts decreasing.
- The “average” polar angle of two particles $\theta_{\text{aver}} = (\pi + \theta_2 - \theta_1)/2$ is inside $\theta_{\text{min}} < \theta_{\text{aver}} < \pi - \theta_{\text{min}}$, where $\theta_{\text{min}} = 1.1$ rad. This condition decreases a systematic error due to angular uncertainties.

A small amount of events has more than two tracks reconstructed in the tracking system. As a rule, this happens because of mistakes of the track reconstruction algorithm or particles coming back from the calorimeter to the drift chamber. In this case all pairs of particles with opposite charges have been checked and an event is accepted if at least one pair satisfies selection criteria.

3 Event separation

The separation of selected collinear events is based on particle momenta measured in the tracking system of the detector. A scatter plot P_+ vs. P_- at the energy $\sqrt{s} = 2 \times 195$ MeV is shown in Fig. 1. One can clearly see regions where electrons, muons and pions are concentrated as well as events at the diagonal of the histogram from cosmic background.

The numbers of events of each type are obtained by minimization of the following likelihood function:

$$\mathcal{L} = - \sum_{\text{events}} \ln \left(\sum_i w_i \cdot f_i(P_-, P_+) \right), \quad \sum_i w_i = 1, \quad (2)$$

where $f_i(P_-, P_+)$ is the probability density function for final particles of the type i which can be electrons, muons, pions or cosmic background to have momenta P_- and P_+ in the tracking system and $w_i = N_i/N_{\text{tot}}$ is the fraction of events of each type in the total number of events.

As an example, we show in Fig. 2 the projection of the two-dimensional approximation onto the negative particle momentum at the the beam energy of 195 MeV.

The selected collinear events consist of 95066 events of the process $e^+e^- \rightarrow e^+e^-$, 9000 events of $e^+e^- \rightarrow \mu^+\mu^-$, 4053 events of $e^+e^- \rightarrow \pi^+\pi^-$ and 4632 events of cosmic background.

4 Pion form factor determination

The cross section of the process $e^+e^- \rightarrow \pi^+\pi^-$ can be written as:

$$\sigma_{\pi^+\pi^-}^{(B)}(s) = \sigma_{\pi^+\pi^-}^{(\text{P.L.})}(s) \cdot |F_\pi(s)|^2, \quad (3)$$

where $\sigma_{\pi^+\pi^-}^{(\text{P.L.})}(s)$ is the cross section of the pointlike pion pair production, $F_\pi(s)$ is the pion electromagnetic form factor. Note that vacuum polarization effects are included in the pion form factor definition and for the calculation of the dispersion integral (1) it is necessary to exclude this contribution and also add the contribution from the process with photon emission by final pions [5]:

$$\sigma_{\pi^+\pi^-(\gamma)}^{(0)}(s) = \sigma_{\pi^+\pi^-}^{(B)}(s) \cdot \lambda(s) \cdot |1 - \Pi(s)|^2, \quad (4)$$

where $\lambda(s)$ is the final state radiation correction, $\Pi(s)$ is the photon polarization operator.

The form factor squared $|F_\pi(s)|^2$ is evaluated from experimental data using the following expression:

$$|F_\pi|^2 = \frac{N_{\pi\pi}}{N_{ee} + N_{\mu\mu}} \frac{\sigma_{ee}^{(B)}(1 + \delta_e)\varepsilon_e(1 - \Delta_B) + \sigma_{\mu\mu}^{(B)}(1 + \delta_\mu)\varepsilon_\mu}{\sigma_{\pi\pi}^{(B)}(1 + \delta_\pi)(1 + \Delta_{H\&D})\varepsilon_\pi}, \quad (5)$$

where N_{ee} , $N_{\mu\mu}$, $N_{\pi\pi}$ are the numbers of electron, muons and pions, obtained in the event separation procedure, $\sigma_{ee}^{(B)}$, $\sigma_{\mu\mu}^{(B)}$, $\sigma_{\pi\pi}^{(B)}$ are Born cross sections, δ_e , δ_μ , δ_π are radiative corrections at chosen selection criteria, $\Delta_{H\&D}$ is the correction for pion losses due to nuclear interaction and decays in flight, ε_e , ε_μ , ε_π are detection efficiencies which depend on the trigger and reconstruction algorithm, Δ_B is the correction for bremsstrahlung of electrons in the beam pipe and detector material.

The cross section of muon pair production, $\sigma_{\mu\mu}^{(B)}$, in the first order of α is known exactly in the frame of QED. By comparing the theoretical and experimental cross sections one can check the event separation procedure as well as the calculation of the radiative corrections which were used in the cross section determination.

The cross section of the process $e^+e^- \rightarrow \mu^+\mu^-$ is evaluated from experimental data using the the following expression:

$$\sigma_{\mu\mu}^{\text{exp}} = \frac{N_{\mu\mu}}{N_{ee}} \frac{\sigma_{ee}^{(B)}(1 + \delta_e)\varepsilon_e(1 - \Delta_B)}{(1 + \delta_\mu)\varepsilon_\mu}, \quad (6)$$

where $N_{\mu\mu}/N_{ee}$ is the experimental ratio of the numbers of muons and electrons obtained in the event separation procedure. For correct analysis the ratio of the experimental and theoretical cross sections $R_\mu = \sigma_{\mu\mu}^{\text{exp}}/\sigma_{\mu\mu}^{\text{theory}}$ should be 1 within experimental uncertainties.

5 Estimation of systematic errors

Various contributions to the systematic uncertainty of the form factor measurement are shown in Table 1. The error caused by the event separation procedure was estimated from the difference between the numbers of events in MC and that obtained by the procedure. The error from the fiducial volume determination was estimated from the precision of the track end-point measurement in the Z-chamber. The reconstruction efficiencies were measured separately for each particle types. The efficiency for electrons was $96.5 \pm 0.1\%$,

Table 1: Contributions to the systematic error.

Source of error	Error, %
Event separation	0.4
Fiducial volume	0.2
Reconstruction efficiency	0.2
Pion loss	0.2
Radiative corrections	0.3
Energy determination	0.3
Bremsstrahlung	0.05
Total	0.7

muons – $96.4 \pm 0.3\%$ and pions – $97.1 \pm 0.4\%$. For the form factor determination of real importance is the difference between these efficiencies which was taken as an estimate of the systematic error. Pion losses due to nuclear interactions in the detector material and decays in flight were determined from the full simulation of the CMD-2 detector [6]. The accuracy of the FLUKA package [7] for the cross sections of nuclear interactions of low momentum pions was used as an estimate of the corresponding systematic error. The calculation of the radiative corrections was based on the work [8] with 0.2% precision for each type of processes. The precision of the collider energy determination was $\Delta E/E \sim 10^{-3}$, resulting in a systematic error in the pion formfactor of about 0.3%. Electrons can lose the large fraction of their energy in the beam pipe and detector material due to photon emission by bremsstrahlung and thus escape selection criteria. The precision of this correction depends on the knowledge of the amount of material with which electrons interact.

6 Discussion

After the event separation procedure and taking into account all corrections at each energy point, the experimental values of the cross section of the process $e^+e^- \rightarrow \mu^+\mu^-$ and pion form factor were obtained as well as the pion cross section for the dispersion integral (1). These values are shown in Table 2.

The obtained ratio $R_\mu = \sigma_{\mu\mu}^{\text{exp}}/\sigma_{\mu\mu}^{\text{theory}}$ is shown in Fig. 3. The difference between the experimental value and theoretical one, averaged over all energies, is $(2.0 \pm 1.3_{\text{stat}} \pm 0.7_{\text{syst}}) \%$. This is the first direct comparison of experimental data and theoretical calculations in the low energy region at the 1% level.

For determination of the pion electromagnetic radius $\langle r_\pi^2 \rangle$ all CMD-2 data on the pion form factor were considered [9, 10]. To describe experimental data, the VDM based model from the previous CMD-2 work on the pion form factor measurement around the ρ -meson [9] was used.

The experimental values of the pion form factor measured in this work and previous experiments [11, 12, 13, 14, 15] are shown in Fig. 4. The electron-positron collider experiments are in good agreement – the average difference between experiments does not

Table 2: Cross section of $e^+e^- \rightarrow \mu^+\mu^-$, electromagnetic form factor of charged pion $|F_\pi|^2$ and cross section of $e^+e^- \rightarrow \pi^+\pi^-$ for the dispersion integral (1). Only statistical errors are shown.

E , MeV	$\sigma_{\mu\mu}^{(B)}$, nb	$ F_\pi ^2$	$\sigma_{\pi\pi(\gamma)}^0$, nb
185	605 ± 16	2.05 ± 0.12	91.8 ± 5.6
195	523 ± 17	1.83 ± 0.12	89.0 ± 5.9
205	476 ± 19	1.98 ± 0.14	100.0 ± 7.0
215	468 ± 14	2.52 ± 0.11	129.7 ± 5.9
225	412 ± 17	2.69 ± 0.15	138.5 ± 7.5
235	373 ± 16	2.83 ± 0.14	144.2 ± 7.3
240	329 ± 21	3.02 ± 0.20	152.4 ± 10.3
250	343 ± 25	3.24 ± 0.24	160.2 ± 11.7
255	336 ± 26	3.83 ± 0.25	186.6 ± 12.4
260	327 ± 25	3.52 ± 0.21	169.2 ± 10.3

exceed 1.5 standard deviations, while the difference with the NA7 experiment is almost 4 standard deviations.

The pion electromagnetic radius depends on the form factor behaviour at low momentum transfers:

$$\langle r_\pi^2 \rangle = 6 \left. \frac{dF_\pi(s)}{ds} \right|_{s=0}.$$

The value obtained from the form factor approximation to the point $s = 0$ is

$$\langle r_\pi^2 \rangle = 0.4219 \pm 0.0010 \pm 0.0012 \text{ fm}^2,$$

where the first error is statistical and the second one is systematic. This value is in good agreement with the result from work [14], $\langle r_\pi^2 \rangle = 0.422 \pm 0.003 \pm 0.013 \text{ fm}^2$. It is also consistent with the result from the NA7 experiment in the spacelike region [16], $\langle r_\pi^2 \rangle = 0.439 \pm 0.008 \text{ fm}^2$.

The hadronic contribution to $a_\mu^{\text{had,LO}}$ from the energy range 390-520 MeV calculated from (1) and measured values of $\sigma_{\pi\pi(\gamma)}^{(0)}$ is $(46.17 \pm 0.98 \pm 0.32) \times 10^{-10}$. This contribution agrees with the value $(48.72 \pm 1.45 \pm 1.51) \times 10^{-10}$ calculated from data of previous experiments [12, 14] and is two times more precise.

7 Conclusion

Results of the measurement of the cross section of the process $e^+e^- \rightarrow \pi^+\pi^-$ in the 370-520 MeV c.m. energy range are presented. A direct test of the QED prediction for the muon pair production cross section has been performed. The pion electromagnetic formfactor has been measured with the world best statistical and systematic accuracy. Using all CMD-2 pion formfactor data the value of the pion electromagnetic radius has been calculated.

This work is partially supported by the Russian Foundation for Basic Research, grants 03-02-16477, 03-02-16280, 04-02-16217, 04-02-16223, 04-02-16434 and 06-02-16156.

References

- [1] T. Kinoshita, B. Nizic and Y. Okamoto, Phys. Rev. D **31**, 2108 (1985).
- [2] M. Davier, S. Eidelman, A. Höcker and Z. Zhang, Eur. Phys. J. C **31**, 503 (2003).
- [3] V.V. Anashin, I.B. Vasserman, V.G.Veshcherevich *et al.*, Preprint INP **84-114**, Novosibirsk, 1984.
- [4] E.V. Anashkin, V.M. Aulchenko, R.R. Akhmetshin *et al.*, PTE **5**, 1 (2006).
- [5] A. Hoefer, J. Gluza, F. Jegerlehner, Eur. Phys. J. C **24**, 51 (2002).
- [6] E.V.Anashkin, A.E.Bondar, N.I.Gabyshev *et al.*, Preprint INP **99-1**, Novosibirsk, 1999.
- [7] A. Fassó, A. Ferrari, S. Roesler *et al.*, eConf **C0303241**, MOMT005 (2003).
- [8] A.B. Arbuzov, G.V. Fedotovitch, F.V. Ignatov *et al.*, Eur. Phys. J. C **46**, 689 (2006).
A.B. Arbuzov, G.V. Fedotovitch, F.V. Ignatov *et al.*, Preprint INP **2004-70**, Novosibirsk, 2004.
- [9] R. R. Akhmetshin, E.V. Anashkin, A.B. Arbuzov *et al.*, Phys. Lett. B **527**, 161 (2002).
R. R. Akhmetshin, E.V.Anashkin, A.B.Arbuzov *et al.*, Phys. Lett. B **578**, 285 (2004).
- [10] V. M. Aulchenko, R.R. Akhmetshin, V.Sh. Banzarov *et al.*, JETP Lett. **82**, 743 (2005).
- [11] A. Quenzer, M. Ribes, F. Rumpf *et al.*, Phys. Lett. B **76**, 512 (1978).
- [12] I. B. Vasserman, P.M. Ivanov, G.Ya. Kezerashvili *et al.*, Yad. Fiz. **33**, 709 (1981).
- [13] S.R. Amendolia, B. Badelek, G. Batignani *et al.*, Phys. Lett. B **138**, 454 (1984).
- [14] L.M. Barkov, A.G. Chilingarov, S.I. Eidelman *et al.*, Nucl. Phys. B **256**, 365 (1985).
- [15] M. N. Achasov, K. I. Beloborodov, A. V. Berdyugin *et al.*, J. Exp. Theor. Phys. **101**, 1053 (2005).
M. N. Achasov, K. I. Beloborodov, A. V. Berdyugin *et al.*, [arXiv:hep-ex/0604052].
- [16] S. R. Amendolia, M. Arik, B. Badelek *et al.*, Nucl. Phys. B **277**, 168 (1986).

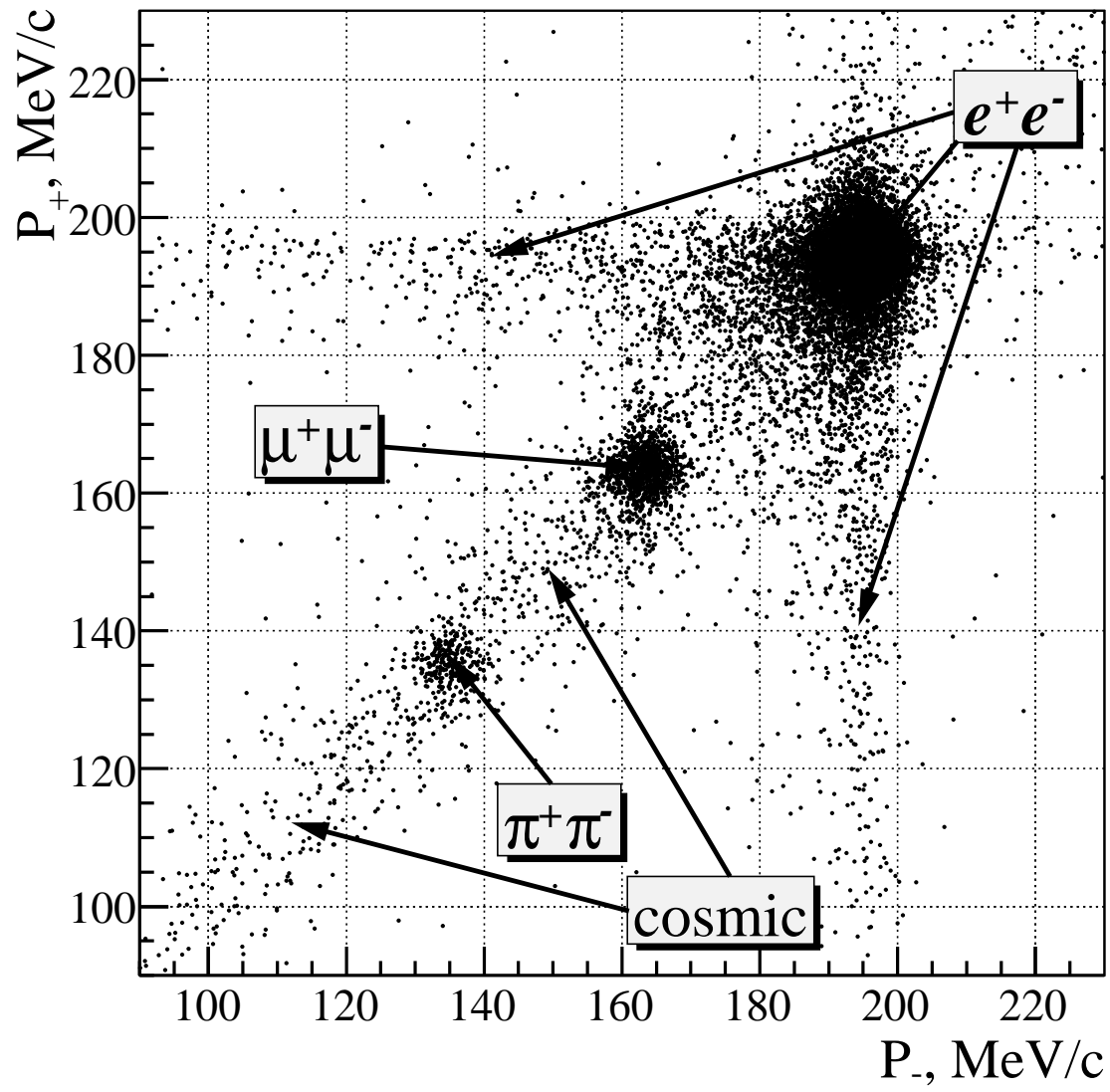


Figure 1: Scatter plot P_+ vs. P_- for experimental data at the beam energy of 195 MeV.

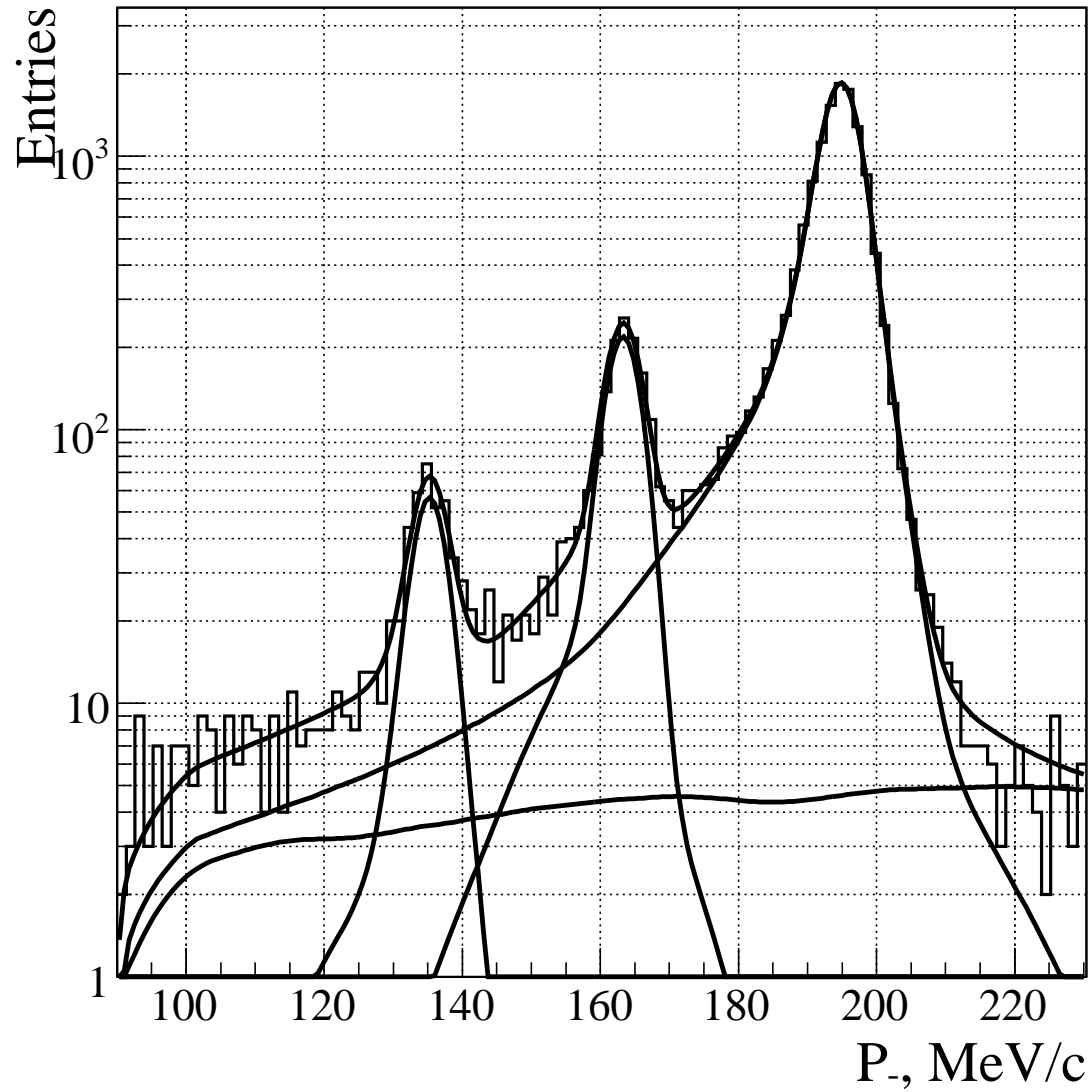


Figure 2: Projection of the two-dimensional approximation of the momentum distribution of experimental data. Curves show contributions from electrons, muons, pions and cosmic background obtained by the event separation procedure.

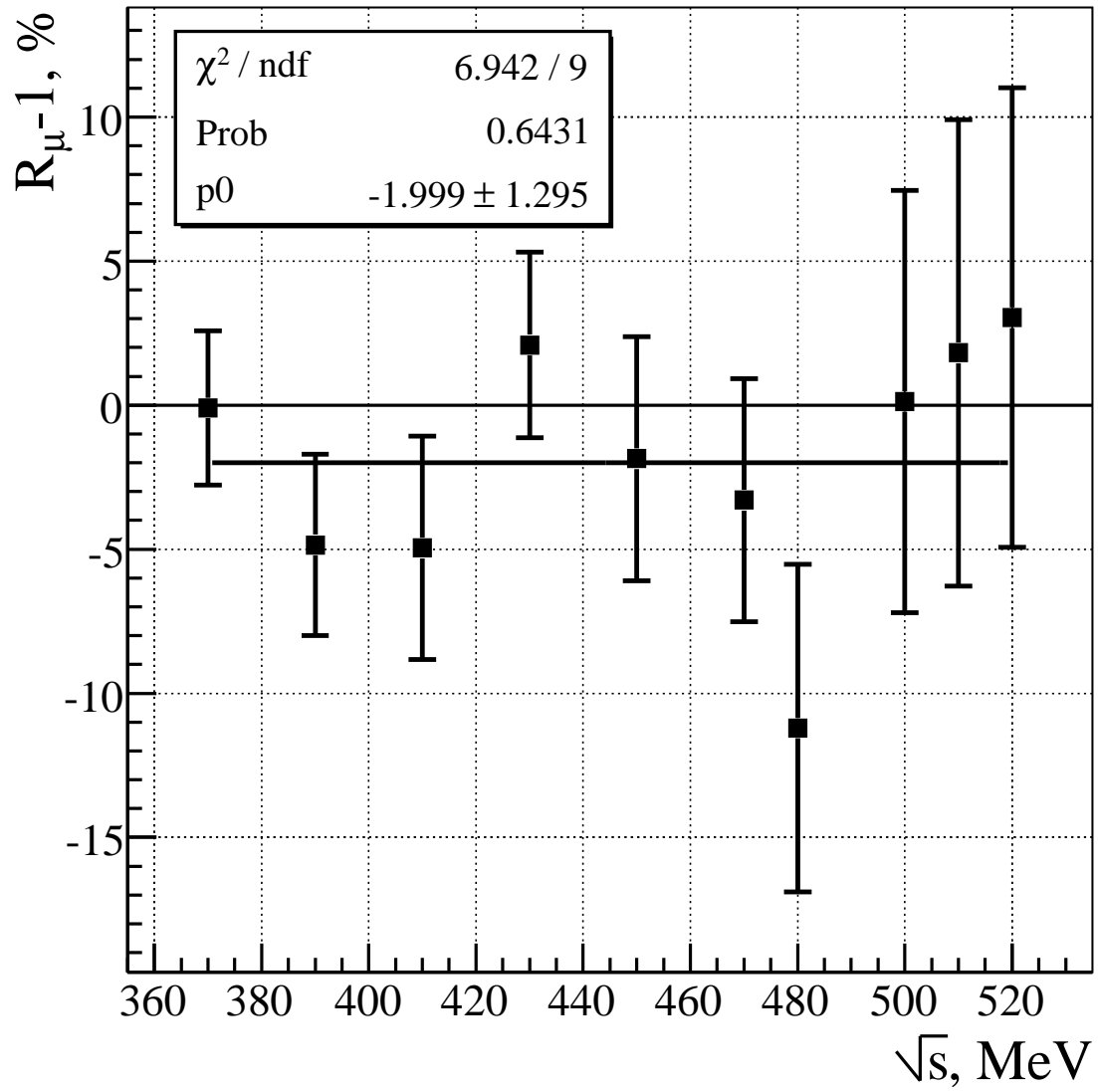


Figure 3: Ratio between experimental and theoretical cross sections of muon pair production R_μ .

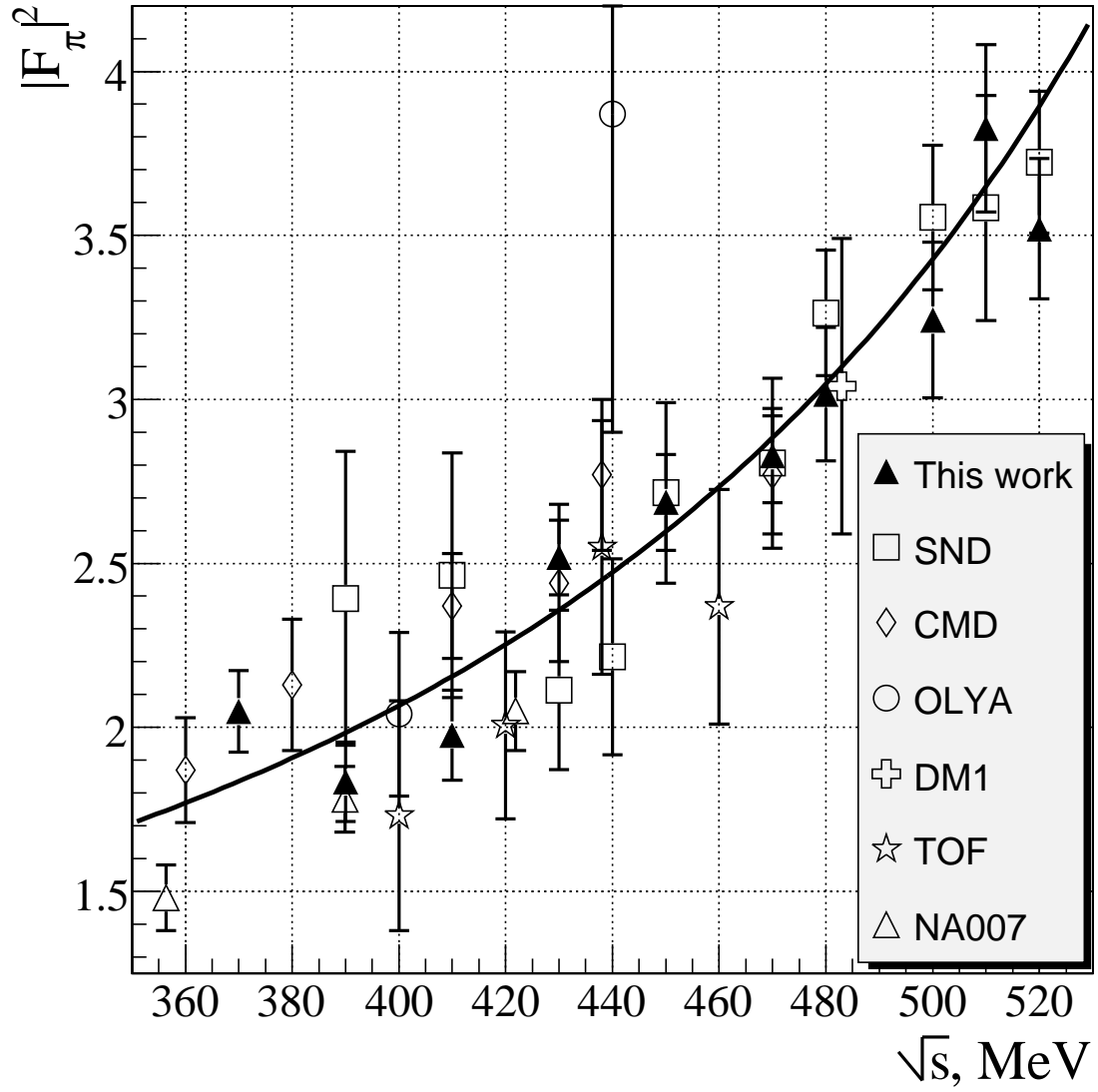


Figure 4: Comparison with other experiments. The curve is the approximation of all CMD-2 pion form factor data.